

Substrate concentration dependence of the diffusion-controlled steady-state rate constant

J. Dzubiella* and J. A. McCammon

NSF Center for Theoretical Biological Physics (CTBP), and

Department of Chemistry and Biochemistry, University of California, San Diego, La Jolla, California 92093-0365

(Dated: June 30, 2018)

The Smoluchowski approach to diffusion-controlled reactions is generalized to interacting substrate particles by including the osmotic pressure and hydrodynamic interactions of the nonideal particles in the Smoluchowski equation within a local-density approximation. By solving the strictly linearized equation for the time-independent case with absorbing boundary conditions, we present an analytic expression for the diffusion-limited steady-state rate constant for small substrate concentrations in terms of an *effective* second virial coefficient B_2^* . Comparisons to Brownian dynamics simulations excluding HI show excellent agreement up to bulk number densities of $B_2^*\rho_0 \lesssim 0.4$ for hard sphere and repulsive Yukawa-like interactions between the substrates. Our study provides an alternative way to determine the second virial coefficient of interacting macromolecules experimentally by measuring their steady-state rate constant in diffusion-controlled reactions at low densities.

I. INTRODUCTION

Simple irreversible reactions of the type $A+B \rightarrow A$ (with A the sink and B the substrates) are commonly found in many (bio)chemical processes, such as fluorescence quenching, enzyme catalysis, polymerization, or colloid and protein aggregation, just to mention a few examples.¹ The key parameter for these processes is the reaction rate constant, a measure for the number of reactions per unit time, first addressed in the pioneering and now classical works of Smoluchowski² and Debye³ decades ago. Since then, various improvements and refinements have been made in predicting the rate constants for diverse reactions,^{1,4,5,6,7,8,9,10,11,12} in particular, including solvent-mediated hydrodynamic interactions (HI) between sink (A) and substrate (B),⁷ or examining effects of a non-zero concentration of the sink particles.^{4,13,14} In most of the previous studies, interactions between the substrate particles were ignored, which is only justified in the case of very weakly interacting substrate particles or at infinite dilution. In recent attempts the influence of the excluded volume of the substrate particles was examined^{15,16} and predicted to yield an increased reaction rate with increasing excluded volume or substrate concentration. Along these lines, Senapati and McCammon¹⁷ also gave evidence for a strong influence of substrate interactions (without HI) on the reaction rate by means of Brownian Dynamics (BD) computer simulations. We tie up to these studies in this work and aim at a systematic examination of the substrate concentration-dependence of the rate constant, while the sinks remain at infinite dilution.

For many of the reactions mentioned above the rate-limiting factor is the diffusional encounter of the reactants, particularly when the subsequent transformation does not involve a large activation barrier. In our work we will focus on the steady-state (long-time) rate of these diffusion-limited or diffusion-controlled reactions. The usual theoretical approach is based on the Smoluchowski equation (SE) which becomes time-independent in the

steady-state. For weakly interacting particles or for small concentrations, the inhomogeneous density profile of the substrates around the sink varies smoothly over distances larger compared to the typical interaction range and well established generalizations of the SE are available,¹⁸ often used for instance for the problem of colloidal sedimentation. The generalized SE employs the osmotic pressure and density-dependent mobility of the interacting particles within a local-density approximation (LDA)¹⁹ which assumes local homogeneity of the density and is justified whenever the density varies slowly in space. Using a simple model with a spherical, isotropically reactive sink particle, we will show that a strictly linearized version of the generalized SE allows us to write down an analytic solution for the first order correction of the rate constant in linear order of substrate concentration. As a result, the correction coefficient is basically given by the second virial coefficient B_2 , the first order correction coefficient in the expansion of the virial equation of state, but must be corrected for HI and is also influenced by the interaction between sink and substrate. Fortunately, most chemical reactions occur at small densities of the reactants so that our result should be valid for a wide range of processes and systems. Despite the simplicity of our model the results are general and should be applicable to more realistic and complicated systems.

In order to examine the range of validity of our theoretical result we perform Brownian dynamics (BD) simulations for different systems in which the interaction between the B particles is varied from hard sphere to attractive and repulsive Yukawa-like interactions, the latter typically found in ionic solutions. The BD simulations do not include HI, which can be accurately treated only by more sophisticated and computationally more expensive means, such as Lattice-Boltzmann methods²⁰ or others.^{21,22,23} However, in comparison to the theory excluding HI we find excellent agreement up to substrate densities $B_2\rho_0 \simeq 0.4$, showing the reliability of our theoretical concept, and proving its applicability to the case when HI can be neglected, i.e. for long-ranged inter-

actions. In principle, our study opens up an alternative way to determine the second virial coefficient of proteins or other particles by measuring the reaction rate in diffusion-limited reactions at small substrate densities.

The paper is organized as follows: In section II we present the basic equations of motion and approximations of our theory and arrive at a first order linear differential equation which can be solved analytically. The solution for the steady-state rate constant and density profile are presented and discussed in section III. A systematic comparison to BD simulations in order to examine the range of validity of our theory follows in section IV. Sec. V concludes our work with a few final remarks.

II. GENERALIZED SMOLUCHOWSKI THEORY

A. Model and basic equations

Let us consider a spherical, isotropically reactive sink particle A with diameter σ_{AA} which reacts with a B particle (substrate) of size $\sigma_{BB} =: \sigma$ when they touch at a center-to-center distance $r = \sigma_{AB} = (\sigma_{AA} + \sigma)/2$. The sinks are at infinite dilution while the B particles have a bulk number density ρ_0 . Furthermore a potential $V_{AB}(r)$ is acting between the sink and the substrate particles. Both A and B are dispersed in a solvent, which is taken into account by a position-dependent diffusion constant $D_0(\mathbf{r})$ of the substrates, reflecting the diffusion of an isolated B particle relative to the A particle. We assume the sink to be completely at rest, which is justified for large sinks $\sigma_{AA} \gg \sigma$. For close distances to A, $D_0(\mathbf{r})$ is determined by the HI between A and B, while for large distances when HI are negligible, we obtain D_0 by the Stokes-Einstein relation

$$D_0(|\mathbf{r}| \rightarrow \infty) = D_0 = (3\beta\pi\eta\sigma)^{-1}, \quad (1)$$

where $\beta^{-1} = k_B T$ is the thermal energy, and η the solvent viscosity.

The time-dependent Smoluchowski equation (SE) for noninteracting particles moving in a potential $V_{AB}(\mathbf{r})$ with a position-dependent diffusion constant $D_0(\mathbf{r})$ is given by

$$\begin{aligned} \partial\rho(\mathbf{r}, t)/\partial t &= -\nabla \cdot \mathbf{J}(\mathbf{r}, t) \\ &= \nabla \cdot D_0(\mathbf{r}) \left[\rho(\mathbf{r}, t) \frac{\beta\partial V_{AB}(\mathbf{r})}{\partial r} + \nabla\rho(\mathbf{r}, t) \right]. \end{aligned} \quad (2)$$

For weak density inhomogeneities, which is always true for small densities or weak interactions, one can introduce substrate interactions by using the generalized Stokes-Einstein relation¹⁸

$$D(\rho) = M(\rho) \frac{d\Pi(\rho)}{d\rho}, \quad (3)$$

where $D(\rho)$ is the collective diffusion coefficient, $M(\rho)$ is the density dependent mobility of the substrate particles,

and $\Pi(\rho)$ the osmotic pressure of the interacting particles. This is a generalized Stokes-Einstein equation in the sense that it generalizes (1) to the case of interacting particles in a homogeneous solution. The mobility $M(\rho)$ is a reciprocal friction and is defined as the proportionality constant between the drift velocity and total force on a Brownian particle (*velocity* = $M(\rho) \times$ *total force*) in a steady-state situation. Within the LDA the generalized Stokes-Einstein relation is applied to the local, position-dependent density $\rho(\mathbf{r})$ of the substrate particles, which we assume to vary smoothly over distances larger compared to the range of the interaction potential. The equation of motion can now be written as¹⁸

$$\begin{aligned} \partial\rho(\mathbf{r}, t)/\partial t &= -\nabla \cdot \mathbf{J}(\mathbf{r}, t) \\ &= \nabla \cdot M(\rho(\mathbf{r}, t), \mathbf{r}) \left[\rho(\mathbf{r}, t) \frac{\partial V_{AB}(\mathbf{r})}{\partial r} + [\nabla\rho(\mathbf{r}, t)] \frac{d\Pi(\rho(\mathbf{r}, t))}{d\rho(\mathbf{r})} \right], \end{aligned} \quad (4)$$

and is a generalization of Eq. (3) to weakly interacting substrate particles. The last term on the rhs of Eq. (4) accounts for the force on a Brownian particle due to an unbalanced osmotic pressure caused by a concentration gradient of interacting particles. In addition, the density-dependent mobility corrects for HI between B particles. Note that for ideal particles $d\Pi/d\rho = k_B T$, and with no HI between B particles $M(\rho(\mathbf{r}), \mathbf{r}) = \beta D_0(\mathbf{r})$ and we find (2) again. To account for reactions at the sink we have to solve Eq. (4) with the boundary condition

$$4\pi\sigma_{AB}^2(\mathbf{r}/r)\mathbf{J}(\mathbf{r}, t)|_{\sigma_{AB}} = -k_i\rho(\mathbf{r}, t)|_{\sigma_{AB}}, \quad (5)$$

where k_i is the intrinsic rate constant. In the limit of fully absorbing boundary conditions, $k_i \rightarrow \infty$, while $\rho(\sigma_{AB}) \rightarrow 0$, and the reaction rate is only limited by the diffusion of the approaching substrates. We are interested in the steady-state solution for the spherically symmetric problem, with which the equation of motion reduces to

$$0 = \frac{\partial}{\partial r} \left(r^2 M(\rho(r), r) \left[\rho(r) \frac{\partial V_{AB}(r)}{\partial r} + \left[\frac{\partial}{\partial r} \rho(r) \right] \frac{d\Pi(\rho(r))}{d\rho(r)} \right] \right) \quad (6)$$

with the boundary conditions for diffusion-controlled reactions

$$4\pi\sigma_{AB}^2 j(\sigma_{AB}) = k\rho_0, \quad (7)$$

and

$$\rho(\sigma_{AB}) = 0 \quad \text{and} \quad \rho(\infty) = \rho_0, \quad (8)$$

where $j(\sigma_{AB})$ is the absolute flux perpendicular through the sink surface at radial distance σ_{AB} from the sink center, and the quantity k is the diffusion-controlled steady-state rate constant which we are interested in.

The osmotic pressure can be expressed in terms of the equation of state, or in general, the virial equation, which is an expansion of the pressure in terms of the particle density ρ . For small densities the series is usually truncated after the second order and the osmotic pressure reads

$$\beta\Pi(\rho) = \rho + B_2\rho^2. \quad (9)$$

Conveniently, the second virial coefficient B_2 can be calculated from the pair interaction $V_{\text{BB}}(\mathbf{r}) =: V(\mathbf{r})$ between the substrates via¹⁹

$$B_2 = \frac{1}{2} \int d\mathbf{r} [1 - \exp(-\beta V(\mathbf{r}))]. \quad (10)$$

The local mobility of the substrates will be in general reduced by a nonzero concentration of other surrounding particles due to HI, and for small densities the correction is linear in ρ , so that we can write

$$M(\rho(r), r) = \beta D_0(r) [1 - \alpha \rho(r)], \quad (11)$$

where $\alpha > 0$ is the first order correction coefficient. In (11) we assume that the HI between A and B, expressed in $D_0(r)$, are independent of the HI between B particles and the resulting mobility can be factorized. For the case of hard spheres with diameter σ it is well established that $\alpha \sigma^{-3} \simeq 3.43$.¹⁸ Substituting (11) and the derivative of (9) with respect to ρ into Eq. (6), integrating and strictly linearizing in ρ_0 we find

$$\frac{C}{D_0(r)r^2} = \rho(r) \left[\frac{\beta \partial V_{\text{AB}}(r)}{\partial r} + \frac{2B_2^* C}{D_0(r)r^2} \right] - \frac{\partial}{\partial r} \rho(r), \quad (12)$$

where we introduced the *effective* second virial coefficient

$$B_2^* = B_2 - \alpha/2, \quad (13)$$

and which has to be solved with boundary conditions Eqs. (7) and (8). The equilibrium pair interaction, described by B_2 , and the dynamic interaction, absorbed in α , compete likewise now in altering the rate of the reaction, and can hence be summarized in the single parameter B_2^* given in (13). This interesting feature will be discussed in more detail in the next section, where the result for k is presented. Eq. (12) is a first order linear differential equation and can be solved analytically. The parameter C is an integration constant, determined by the boundary conditions, and is related to the rate constant with $C = \rho_0 k / 4\pi$.

B. Result for the steady-state rate constant

From the linearized solution of (12) we arrive at the result for the diffusion-controlled steady-state rate constant valid for small densities (or weak interactions)

$$k = k_D \left[1 + B_2^* \rho_0 \frac{I(\infty)}{I_1(\infty)} \right], \quad (14)$$

where k_D is the classical result of Debye³ for ideal or infinitely diluted substrates in a nonzero potential $V_{\text{AB}}(r)$

$$k_D = \left\{ \int_{\sigma_{\text{AB}}}^{\infty} dr \frac{\exp[\beta V_{\text{AB}}(r)]}{4\pi D_0(r)r^2} \right\}^{-1} = \{I_1(\infty)\}^{-1} \quad (15)$$

and

$$I(r) = 2 \frac{I_0(r)I_1(r) - I_2(r)}{I_1(\infty)} \quad (16)$$

with the integrals

$$I_0(r) = \int_{\sigma_{\text{AB}}}^r dr' \frac{1}{4\pi D_0(r')r'^2}, \quad (17)$$

$$I_1(r) = \int_{\sigma_{\text{AB}}}^r dr' \frac{\exp[\beta V_{\text{AB}}(r')]}{4\pi D_0(r')r'^2}, \quad (18)$$

and

$$I_2(r) = \int_{\sigma_{\text{AB}}}^r dr' \frac{\exp[\beta V_{\text{AB}}(r')] I_0(r')}{4\pi D_0(r')r'^2}, \quad (19)$$

which are functions depending on the particular interaction $V_{\text{AB}}(r)$ and the position-dependent diffusion constant $D_0(r)$. When interactions between A and B can be neglected, namely $D_0(r) = D_0$, and $V_{\text{AB}}(r) = 0$, it follows $I(\infty)/I_1(\infty) = 1$, and the result for the steady-state rate constant reduces to

$$k = 4\pi D_0 \sigma_{\text{AB}} (1 + B_2^* \rho_0), \quad (20)$$

which for noninteracting particles or at infinite dilution of species B gives the classical Smoluchowski result²

$$k_0 = 4\pi D_0 \sigma_{\text{AB}}. \quad (21)$$

The constant $I(\infty)/I_1(\infty)$ in (14) depends on the particular interaction $V_{\text{AB}}(r)$ and $D_0(r)$ between A and B particles, but is always close to 1 for Lennard-Jones or Yukawa like interactions typically found in solutions, and a $D_0(r)$ for instance given by the Oseen tensor.⁶ The major contribution to the density correction stems from the effective second virial coefficient (13), which is a corrected second virial coefficient for the dynamic situation and features the following interesting trends for the steady-state rate constant. Generally $\alpha > 0$, imposing that HI will decrease the substrate mobility. However, if the substrate-substrate interaction is strongly repulsive, $B_2 > \alpha/2$, so that B_2^* is positive, an enhanced reaction rate is predicted compared to the noninteracting case. On the contrary, a mainly attractive pair interaction will in general lead to a negative B_2^* and decrease the reaction rate. For long-ranged interactions $|B_2|$ may be an order of magnitude larger than $\alpha/2$ and HI can be neglected, such that $B_2^* \simeq B_2$. When the repulsive interaction leads to a B_2 comparable to $\alpha/2$, both contributions can cancel each other and the reaction rate just changes little or not at all with increasing (small) density or (weak) interaction. For instance, for the repulsive hard sphere case the effective second virial coefficient $B_2^* \sigma^{-3} \simeq 2.09 - 3.43/2 \simeq 0.38$ is small due to a slowing of the diffusion of the substrates which is comparable to the effects of the enhanced osmotic pressure in the system, leading just to a minor increase of the rate constant with density. Our theory is in agreement with previous work^{15,16} where the excluded volume of the substrates is predicted to lead to an enhanced reaction rate (excluding HI). It is worth mentioning that B_2^* is half of the coefficient of the linear first

order correction in ρ_0 of the collective diffusion coefficient of the substrates in bulk solution, latter evident from the generalized Stokes-Einstein relation (3). The range of validity of (14) will be examined in section III for hard sphere and repulsive and attractive Yukawa interactions excluding HI.

C. Result for the density profile

The general solution for the diffusion-controlled steady-state density profile in linear order in ρ_0 reads

$$\rho(r) = \rho_0 \frac{k_D I_1(r)}{\exp[\beta V_{AB}(r)]} \left(1 + B_2^* \rho_0 \left[\frac{I(\infty)}{I_1(\infty)} - \frac{I(r)}{I_1(r)} \right] \right) \quad (22)$$

In order to better identify how the substrate interactions affect the density profiles we rewrite the solution for the case of no interactions between substrate and sink, $D_0(r) = D_0$ and $V_{AB}(r) = 0$:

$$\rho(r) = \rho_{id} \left(1 + B_2^* \rho_0 \frac{\sigma_{AB}}{r} \right), \quad (23)$$

where

$$\rho_{id}(r) = \rho_0 \left(1 - \frac{\sigma_{AB}}{r} \right) \quad (24)$$

is the classical result for ideal or infinitely diluted substrate particles when $V_{AB} = 0$ and $D_0(r) = D_0$.^{2,4} Eq. (23) predicts that a positive B_2^* will enhance the substrate density close to the absorbent due to a higher (positive) bulk pressure of the B particles compared to the noninteracting case. This is opposite to the case of negative B_2^* (mainly attractive interactions) where a depletion of B particles takes place close to A due to a negative bulk pressure, and/or a larger immobility of the approaching substrates. Comparing these trends to the rate constant (14) we conclude that an enhanced or lower density close to the sink increases or decreases the reaction rate, respectively, at least for small densities. These predictions will be examined in the next section with BD simulations.

III. BROWNIAN DYNAMICS SIMULATION

A. Simulation details

For a verification of the theory in the previous section we perform standard Brownian Dynamics simulations using the integration technique of Ermak and McCammon,²⁴ and in addition accounting for hard sphere overlap.²⁵ In order to conduct a clear and transparent comparison to the theoretical result we neglect HI in the BD simulations. An accurate treatment of HI is only given by more sophisticated and computationally expensive techniques, such as Lattice-Boltzmann²⁰ or others.^{21,22,23} Thus, in the following $D_0(r) = D_0$ given

by (1), and $B_2^* = B_2$. In the BD simulations, the steady-state rate constant is determined by calculating the survival probability $S(t)$ of the sink particle A in the steady-state, which is given by

$$S(t) = \exp(-k\rho_0 t) \quad (25)$$

in the presence of reactive B particles with bulk density ρ_0 . In our simulation model, the sink is fixed in the center of the periodically repeated, cubic simulation box with length L . Substrate (B) particles react with the sink (A) as soon they touch it, which happens at a center-to-center distance $r_{AB} = \sigma_{AB}$. The trajectory of a B particle is terminated after reaction. The survival probability can be easily measured by forming an histogram of the times between two reactions and normalize it with respect to the number of total reactions in one simulation. To account for the steady-state case and simulate a fixed density ρ_0 far away from the sink, the annihilated B particle is reinserted randomly at a position close ($r_{AB} > 0.45L$) to the box edges. Due to the long range of the steady-state density-profile (23), finite size effects can be large for too small box sizes for all densities and have been analyzed by performing finite size scaling simulations. Eventually the box lengths used in our simulations range from $L = 50\sigma$ up to $L = 200\sigma$ depending on density and interaction of the B particles. This involved simulations of $N_B = 1000 - 30000$ substrate particles using 5×10^7 to 2×10^5 timesteps. The integration timestep was chosen to be $0.003\tau_B$, where $\tau_B = \sigma^2/D_0$ is a typical Brownian timescale in the simulation. Verlet-neighbor lists were used to optimize computational time.²⁶ Densities up to $B_2\rho_0 \lesssim 1$ could be simulated; for larger densities the system size and statistical errors become too large for reasonable output.

B. Systems

In order to perform a systematic comparison to the theoretical results we consider four different systems, I, II, III, and IV which differ in the interaction between A and B, and B and B particles. In all systems the interactions are in general given by

$$\beta V_{ij}(r) = \beta V_{HS}(r_{ij}) + U_{ij} \frac{\sigma_{ij}}{r_{ij}} \exp[-\kappa(r_{ij} - \sigma_{ij})] \quad (26)$$

where βV_{HS} is the hard sphere interaction

$$\beta V_{HS} = \begin{cases} \infty & \text{for } r_{ij} \leq \sigma_{ij}; \\ 0 & \text{else,} \end{cases} \quad (27)$$

and the second term in (26) is a Yukawa interaction with energy scale U_{ij} , inverse screening length κ , and $i, j = A, B$. κ will be fixed to $\kappa\sigma = 1$ in all our four systems. We also fix the length scale to $\sigma_{AB} = 1.5\sigma$, which is given when the sink particle is twice as large as the substrate particle $\sigma_{AA} = 2\sigma$. We note already that

| System | U_{AB} | U_{BB} | σ_{AB}/σ | $B_2\sigma^{-3}$ | $I(\infty)/I_1(\infty)$ |
|--------|----------|----------|----------------------|------------------|-------------------------|
| I | 0.0 | 0.0 | 1.5 | 2.09 | 1.00 |
| II | 0.0 | 1.0 | 1.5 | 13.32 | 1.00 |
| III | -1.0 | 1.0 | 1.5 | 13.32 | 1.11 |
| IV | 0.0 | -0.5 | 1.5 | -4.62 | 1.00 |

TABLE I:

we have simulated selected densities for all four systems for two other sink sizes, namely $\sigma_{AB} = \sigma$ and $\sigma_{AB} = 2\sigma$, and did not find any deviation from the results later in the work. For high asymmetries $\sigma_{AA} \gg \sigma$, which is the more realistic case, the BD simulations unfortunately become computationally expensive due to a large number of substrate particles which have to be simulated. Note again that the range of the steady-state density profile increases essentially linearly with σ_{AB} , see Eq. (23); however, we stress that this does not affect our theoretical result (14) which should be valid for all size ratios, and we have chosen smaller sink sizes only for computational convenience.

In system I we simply consider $U_{ij} = 0$, in which case all interactions are hard sphere like. The second virial coefficient for HS is $B_2\sigma^{-3} = 2\pi/3 \simeq 2.09$. In system II Yukawa-like repulsion $U_{BB} = 1$ is added between the substrate particles. The second virial coefficient increases to a total of $B_2\sigma^{-3} \simeq 2\pi/3 + 11.23 \simeq 13.32$. In system III a Yukawa attraction is added between sink (A) and substrate (B) particles, $U_{AB} = -1$, while keeping the B-B interaction as in system II. Finally, in system IV we choose $U_{AB} = 0$, no interaction between A and B, but here we focus on attraction between the B particles, $U_{BB} = -0.5$, resulting in a total negative second virial coefficient $B_2\sigma^{-3} \simeq -4.62$. The system parameters and corresponding values of the second virial coefficient and the constant $I(\infty)/I_1(\infty)$ are summarized in Tab. 1.

Typical examples of the calculated survival probabilities (25) are shown in Fig. 1 for systems I, II, and IV on a logarithmic ordinate and show linear behavior for all times within the uncertainty of the statistics. The density for system I (hard spheres) is chosen to be very small ($B_2\rho_0 = 0.001$) and the survival probability matches with the classical theoretical result $S(t) = \exp(-k_0\rho_0 t)$, also shown in Fig.1 as dashed line. As expected from the theory, a positive or negative B_2 (systems II and IV) increases or decreases the rate constant, respectively, as is indicated by an increased or decreased absolute slope of the $S(t)$ curves. Linear fits through these curves determine our 'experimental' values of the rate constant for all systems, while the regression coefficient of the fitting procedure provides the error bars.

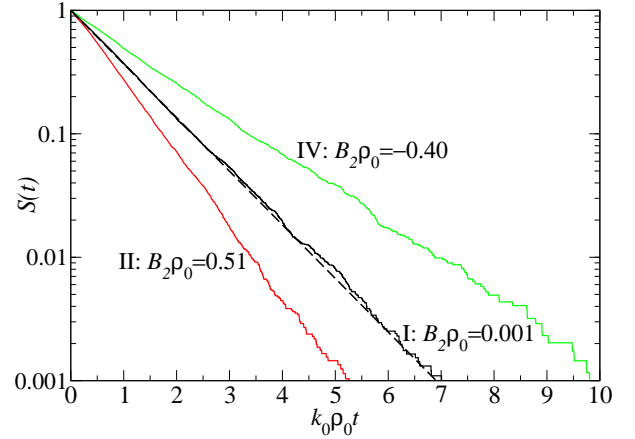


FIG. 1: Typical examples for the survival probability $S(t)$ on a logarithmic scale versus time scaled by the ideal substrate rate constant k_0 (21) and substrate bulk density ρ_0 . The straight dashed line is the ideal result $S(t) = \exp(-k_0\rho_0 t)$, while the noisy data are BD simulation results for chosen densities in systems I, II, and IV.

C. Results

Examples of the density profiles for system I, II, and IV are shown in Fig. 2 compared to the theoretical prediction (23) and are in very good agreement. The density for system I is in the very dilute region ($B_2\rho_0 = 0.001$) and the profile matches the $1 - \sigma_{AB}/r_{AB}$ behavior (24) for ideal substrate particles. Further on, the predicted density increase (decrease) around the sink by repulsive (attractive) substrate interactions is verified by the BD simulations. All observed density profiles exhibit a very small but nonvanishing density value at contact $\rho(\sigma_{AB}) \simeq 0.05$, showing that the assumption $\rho(\sigma_{AB}) = 0$ for absorbing boundary conditions in the theory is justified, but not perfect. This contact value increases (decreases) slightly with positive (negative) B_2 .

Results for the rate constant are shown in Fig. 3 where we plot the steady-state rate constant scaled by the ideal rate constant k_0 given by (21) versus the substrate density scaled by the second virial coefficient B_2 , which can be different for each system, see Tab. 1. Note again that we neglect III in our simulations, such that $\alpha = 0$ and $D_0(r) = D_0$, and $B_2^* = B_2$ in the theory. We find excellent agreement to the theory (lines) within the statistical uncertainties of the simulation for the systems with repulsive substrate interaction (I-III) up to densities $B_2\rho_0 \simeq 0.4$. For system I, the hard sphere case, the non-linear regime takes over for larger densities and the theoretical prediction underestimates the rate constant. For systems II and III we still find good agreement (theory within the error bars) till up to $B_2\rho_0 \simeq 0.7$. This agree-

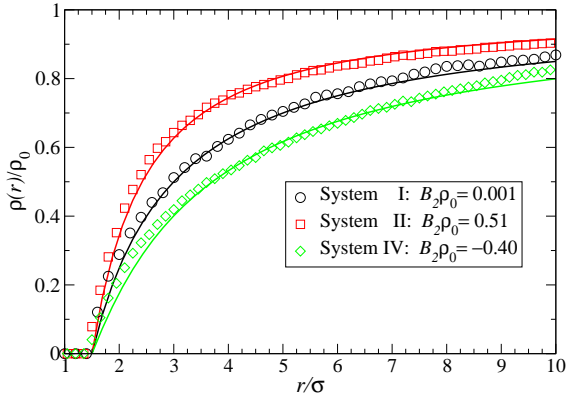


FIG. 2: Steady-state density profiles $\rho(r)$ of the substrates around the sink particle from BD simulations (symbols) and theory (lines) according to Eq. (23) for three different parameter sets. r is the distance from the center of the sink. The circles are close to the infinite dilution limit (24), while squares and diamonds are for positive and negative B_2 for nonzero bulk densities ρ_0 , respectively.

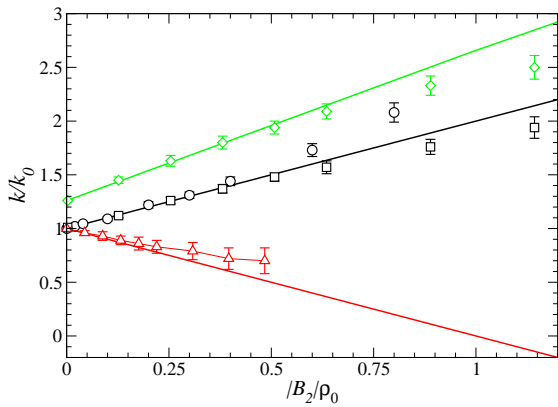


FIG. 3: Dimensionless reaction rate k/k_0 from BD simulations (symbols) and theory (lines, Eq.(14)) versus density of the substrate particles for the four different systems I (circles), II (squares), III (diamonds), and IV (triangles). Note that the density is scaled by the corresponding second virial coefficient, see Tab. I, that is why the theoretical curves for I and II are on top of each other and have the same absolute slope as the curve for IV.

ment for a larger density range as compared to HS could be anticipated since for soft repulsive interactions it is known that higher order virial coefficients (B_3 , and so on) are less important even for higher densities.²⁷ However, for larger densities the shortcomings of the linearized Smoluchowski equation also take their effects. In the sys-

tem with attractive substrate interactions (IV) the agreement is good only for smaller densities ($B_2\rho_0 \lesssim 0.20$). Equilibrium statistics has shown that for attractive interactions, a LDA approach usually fails to give an accurate description of the system behavior even for weak interactions, which could also be the case here. Secondly, finite size effects in the simulation are larger due to a longer ranged density profile (23) and cannot be excluded to explain the discrepancies for larger densities. The theoretical curves for I and II are on top of each other and have the same absolute slope as the data for IV because the density is scaled by the corresponding B_2 . For zero density the curves for I, II, and IV intersect at $k/k_0 = 1$ which is the classical ideal gas limit for no interactions between B and B, and A and B. Curve III intersects at a larger value $k/k_0 \simeq 1.26$ due to the additional A-B interaction in this system. This is also the main reason for the increased absolute slope compared to I, II, and IV, but additionally the constant $I(\infty)/I_1(\infty) \simeq 1.1$ is enhanced by the attractive A-B interaction in this system.

IV. CONCLUDING REMARKS

In conclusion we have derived an analytic expression for the density profile and rate constant for weakly interacting substrate particles for the steady-state case of diffusion controlled reactions. For this purpose we used the Smoluchowski equation, which was generalized within a LDA to account for the osmotic pressure and HI of the interacting substrates. A comparison to BD simulations excluding hydrodynamic interactions (accounted for in the theory by $\alpha = 0$) showed excellent agreement for densities up to $B_2\rho_0 \simeq 0.4$ for repulsive interactions, and up to $B_2\rho_0 \simeq 0.20$ for Yukawa-like attractions. Our BD simulations do not include HI but support our theoretical concept and prove its validity when HI can be neglected, i.e. for long-ranged interactions. We are confident that our theoretical treatment is valid also in the general case including HI; when the density-profiles of the substrates are slowly varying in space, the correlations in the system are usually well approximated by those in the bulk, even in the dynamic case.¹⁸ However, a verification of our theory including HI is highly desired and abandoned to future work, where the HI need to be treated by accurate means.

In principle, our study provides an alternative way to estimate the second virial coefficient of interacting macromolecules experimentally by measuring their steady-state rate constant in diffusion-controlled reactions at low densities. In such experiments, the effective sink-substrate interaction has to be known (e.g. by measuring the infinite dilution limit of the rate constant) and the hydrodynamic quantities $D_0(r)$ and α must be approximated, e.g. by using the Oseen tensor,⁶ and approximating the substrate particles by hard spheres with an effective hydrodynamic radius, respectively.¹⁸

The generalized Smoluchowski equation used in our

work can also be understood as a LDA in the recently proposed framework of dynamic density functional theory (DDFT),²⁸ where equilibrium correlations are used to approximate the dynamical correlation in a Brownian system. It was shown by BD simulations that DDFT including more sophisticated approximations than LDA works well in the case of dense one²⁸ and three-dimensional hard spheres,²⁹ and three-dimensional particles with very soft interactions,^{30,31,32} and seems to provide a powerful tool to extend our work to more strongly correlated systems, i.e. nucleating or aggregating colloids, polymerization, or binding in crowded protein solutions.³³

Finally, we hope that our approach will shed some light on interpretations of experimental rate constant measurements³⁴ and will be useful in extend-

ing existing works on the time-dependence of the rate constant,^{5,6,35} crowding effects in reactions,^{10,11} finite sink concentration,^{4,13,14} or anisotropic reactivity^{6,36} to the case of interacting substrate particles.

Acknowledgment

The authors are grateful to Christos N. Likos for a critical reading of the manuscript and Sanjib Senapati for useful discussions. J.D. acknowledges financial support from a DFG Forschungsstipendium. Work in the McCammon group is supported by NSF, NIH, HHMI, CTBP, NBCR, and Accelrys, Inc.

* e-mail address: jdzubiella@ucsd.edu

¹ S. A. Rice, *Diffusion-Limited Reactions* (Elsevier, Amsterdam, 1985).
² M. von Smoluchowski, Phys. Z. **17**, 557 (1916).
³ P. Debye, Trans. Elektrochem. Soc. **82**, 265 (1942).
⁴ B. U. Felderhof and J. M. Deutch, J. Chem. Phys. **64**, 4551 (1976).
⁵ S. H. Northrup and J. T. Hynes, J. Chem. Phys. **71**, 871 (1979).
⁶ S. H. Northrup, S. A. Allison, and J. A. McCammon, J. Chem. Phys. **80**, 1517 (1984).
⁷ D. F. Calef and J. F. Deutch, Annu. Rev. Phys. Chem. **34**, 493 (1983).
⁸ G. O. Berg and H.-P. von Hippel, Annu. Rev. Biophys. Biophys. Chem. **14**, 131 (1985).
⁹ W. Dong, F. Baros, and J. C. Andre, J. Chem. Phys. **91**, 4643 (1989).
¹⁰ H.-X. Zhou and A. Szabo, J. Chem. Phys. **95**, 5948 (1991).
¹¹ K. Ibuki and M. Ueno, J. Chem. Phys. **107**, 6594 (1997).
¹² S. Yang, J. Kim, and S. Lee, J. Chem. Phys. **111**, 10119 (1999).
¹³ A. Szabo, R. Zwanzig, and N. Agmon, Phys. Rev. Lett. **61**, 2496 (1988).
¹⁴ I. V. Gopich, A. M. Berezhkovskii, and A. Szabo, J. Chem. Phys. **117**, 2987 (2002).
¹⁵ Y. Jung and S. Lee, J. Phys. Chem. A **101**, 5255 (1997).
¹⁶ J. Lee, J. Sung, and S. Lee, J. Chem. Phys. **113**, 8686 (2000).
¹⁷ S. Senapati, C. F. Wong, and J. A. McCammon, J. Chem. Phys. **121**, 7896 (2004).
¹⁸ J. Dhont, *An Introduction to Dynamics of Colloids* (Else-

vier, Amsterdam, 1996).
¹⁹ J.-P. Hansen and I. R. McDonald, *Theory of Simple Liquids* (Academic Press, London, 1986), 2nd ed.
²⁰ J. Stat. Phys. **107** (2002), special issue.
²¹ A. Malevanets and R. Kapral, J. Chem. Phys. **110**, 8605 (1999).
²² K. Tucci and R. Kapral, J. Chem. Phys. **120**, 8262 (2004).
²³ H. Tanaka and T. Araki, Phys. Rev. Lett. **85**, 1338 (2000).
²⁴ D. L. Ermak and J. A. McCammon, J. Chem. Phys. **69**, 1352 (1978).
²⁵ B. Cichocki and K. Hinsen, Physica A **187**, 133 (1992).
²⁶ M. P. Allen and D. J. Tildesley, *Computer Simulation of Liquids* (Clarendon Press, Oxford, 1987).
²⁷ C. N. Likos, Phys. Rep. **348**, 267 (2001).
²⁸ U. M. B. Marconi and P. Tarazona, J. Chem. Phys. **110**, 8032 (1999).
²⁹ M. Schmidt, P. Royall, and J. Dzubiella, to be published.
³⁰ J. Dzubiella and C. N. Likos, J. Phys.: Condens. Matter **15**, L147 (2003).
³¹ F. Penna, J. Dzubiella, and P. Tarazona, Phys. Rev. E **68**, 061407 (2003).
³² A. J. Archer and R. Evans, J. Chem. Phys. **121**, 4246 (2004).
³³ H.-X. Zhou, J. Mol. Recog. **17**, 368 (2004).
³⁴ M. Chaplin and C. Bucke, *Enzyme Technology* (Cambridge Univ. Press, Cambridge, 1990).
³⁵ V. V. Beijeren, W. Dong, and L. Boquet, J. Chem. Phys. **114**, 6265 (2001).
³⁶ H.-X. Zhou, Biophys. J. **64**, 1711 (1993).